



HAL
open science

Structure, dielectric and piezoelectric properties of $\text{Pb}[(\text{Zr}_{0.45}, \text{Ti}_{0.5})(\text{Mn}_{0.5}, \text{Sb}_{0.5})_{0.05}]\text{O}_3$ ceramics

Louanes Hamzioui, Fares Kahoul, Ahmed Boutarfaia, Abderezak Guemache,
Michel Aillerie

► To cite this version:

Louanes Hamzioui, Fares Kahoul, Ahmed Boutarfaia, Abderezak Guemache, Michel Aillerie. Structure, dielectric and piezoelectric properties of $\text{Pb}[(\text{Zr}_{0.45}, \text{Ti}_{0.5})(\text{Mn}_{0.5}, \text{Sb}_{0.5})_{0.05}]\text{O}_3$ ceramics. *Processing and Application of Ceramics*, 2020, 14 (1), pp.19-24. 10.2298/PAC2001019H . hal-02631233

HAL Id: hal-02631233

<https://hal.science/hal-02631233v1>

Submitted on 13 Jan 2021

HAL is a multi-disciplinary open access archive for the deposit and dissemination of scientific research documents, whether they are published or not. The documents may come from teaching and research institutions in France or abroad, or from public or private research centers.

L'archive ouverte pluridisciplinaire **HAL**, est destinée au dépôt et à la diffusion de documents scientifiques de niveau recherche, publiés ou non, émanant des établissements d'enseignement et de recherche français ou étrangers, des laboratoires publics ou privés.



Structure, dielectric and piezoelectric properties of $\text{Pb}[(\text{Zr}_{0.45}, \text{Ti}_{0.5})(\text{Mn}_{0.5}, \text{Sb}_{0.5})_{0.05}]\text{O}_3$ ceramics

Louanes Hamzioui^{1,2,*}, Fares Kahoul^{1,2}, Ahmed Boutarfaia², Abderezak Guemache¹, Michel Aillerie³

¹Université Mohamed Boudiaf M'sila, Faculté de Soocl Commun, M'sila 28000, Algeria

²Laboratoire de Chimie Appliquée, Université de Biskra, BP.145, RP-Biskra 07000, Algeria

³LMOPS - Laboratoire Matériaux Optiques, Photonique et Systèmes, University of Lorraine, 57070 Metz, France

Received 5 April 2019; Received in revised form 16 August 2019; Received in revised form 25 November 2019;

Accepted 21 January 2020

Abstract

This study describes structure, dielectric and piezoelectric properties of $\text{Pb}[(\text{Zr}_{0.45}, \text{Ti}_{0.5})(\text{Mn}_{0.5}, \text{Sb}_{0.5})_{0.05}]\text{O}_3$ (PZT-PMS) ceramics prepared by conventional mixed-oxide route and sintered at up to 1180 °C. The prepared ceramics was characterized by X-ray diffraction and scanning electron microscopy. The piezoelectric constants, dielectric constant, Young's modulus and electromechanical factors were measured in broad temperature range. The results showed that the PZT-PMS ceramics is composed of tetragonal and rhombohedral phases and has the average grain size of about 1 μm . The $\text{Pb}[(\text{Zr}_{0.45}, \text{Ti}_{0.5})(\text{Mn}_{0.5}, \text{Sb}_{0.5})_{0.05}]\text{O}_3$ ceramics has excellent dielectric and piezoelectric properties for wide practical applications. Thus, planar coupling factor of 0.70, poled dielectric constant of 8215, the Curie temperature of 345 °C and dielectric loss of 6% were attained in the PZT-PMS ceramics sintered at 1180 °C.

Keywords: Mn/Sb doped PZT, microstructure, dielectric properties, piezoelectric properties

I. Introduction

As extensively reported in the last decades [1,2], $\text{Pb}(\text{Zr}_{1-x}\text{Ti}_x)\text{O}_3$ (PZT) ceramics has wide applications in the area of science and technology. Currently PZT ceramics has been widely used in motors, piezoelectric actuators, piezoelectric transformers, ultrasonic vibrator, filter, blue luminescence, resonator, and medical applications [3,4]. The morphotropic phase boundary (MPB) separating the Zr-rich rhombohedral symmetry from Ti-rich tetragonal symmetry contributes to the highest piezoelectric response, which is located around Zr/Ti 52/48 in binary PbZrO_3 - PbTiO_3 system [5]. These ceramic properties are strongly influenced by the density and microstructure which depend on the procedure of synthesis and the powder processing [6].

PZT perovskite structure is distorted below 350 °C (the Curie temperature) [7], when this structure has Zr^{4+} in position B (the center of the unit cell), and has

PbZrO_3 rhombohedral phase. However, when Ti_4^+ occupies the B site of a structure, the tetragonal phase of PbTiO_3 appears [8].

Classically, the electrical properties of PZT ceramics are modulated by the incorporation of small amounts of cations (doping), typically 0.5–2 mol%. Modification of PZT with suitable substitutions of single or multiple cations at Pb^{2+} and $\text{Zr}^{4+}/\text{Ti}^{4+}$ sites helps in enhancing its physical and electrical properties. There are two principal categories of dopants [9,11]. Donor dopants (softeners) which are higher valence substitutes like Nb^{5+} or Sb^{5+} in the place of $(\text{Zr}^{4+}/\text{Ti}^{4+})$ or Gd^{3+} or Eu^{3+} in the place of Pb^{2+} . They cause the following changes of the PZT characteristics: higher dielectric constant and losses (at room temperature), higher charge coefficient d_{31}/d_{33} , much lower mechanical quality factor Q_m and easy depolarization by mechanical stress. The excess of positive charge in the soft PZT is compensated by lead vacancies. Acceptor dopants (hardeners) are lower valence substitutes like Mg^{2+} or Fe^{3+} (B-site) or Na^+ (A-site). They cause the following changes of

*Corresponding author: tel: +213661752635, e-mail: louanes.hamzioui@univ-Msila.dz

the PZT characteristics: lower dielectric constant and losses (at room temperature), lower d_{33} , much higher mechanical Q_m and difficult depolarization by mechanical stress. The lack of positive charge in the hard PZT is compensated by oxygen vacancies. The complex doping of two or more elements is expected to combine the properties of donor doped and/or acceptor doped PZT, which could exhibit better stability or improved piezoelectric and dielectric properties than those of the single element doped PZT [12,16]. Manganese could be introduced into the PZT-based ternary piezoceramics to improve the bulk density causing the combinatorial effect of “hardening” and “softening” [17]. As reported for Mn-doped PZT-based piezoceramics [18,19], both an increment of d_{33} and Q_m could be achieved with a certain content of Mn, but the mechanical properties have been rarely investigated.

In this study, $\text{Pb}[(\text{Zr}_{0.45}, \text{Ti}_{0.5})(\text{Mn}_{0.5}, \text{Sb}_{0.5})_{0.05}]\text{O}_3$ ternary piezoelectric ceramics was investigated by varying the firing temperature. The first purpose of the present study is to determine the width of tetragonal and rhombohedral co-existence phase region. The second objective of this work resides in detail study of the dielectric and piezoelectric properties of $\text{Pb}[(\text{Zr}_{0.45}, \text{Ti}_{0.5})(\text{Mn}_{0.5}, \text{Sb}_{0.5})_{0.05}]\text{O}_3$ ceramics near the MPB.

II. Experimental details

$\text{Pb}[(\text{Zr}_{0.45}, \text{Ti}_{0.5})(\text{Mn}_{0.5}, \text{Sb}_{0.5})_{0.05}]\text{O}_3$ (hereafter abbreviated as PZT-PMS) was synthesized by solid state reaction using oxide precursors: Pb_3O_4 (99.9% M/S Aldrich chemicals, USA), TiO_2 (98.9%, Travancore Titanium Products), ZrO_2 (99.9% M/S Aldrich chemicals, USA), Sb_2O_3 (99%, Biochem) and Mn_2O_3 (99%, Acros). The precursor powders were dispersed in acetone and mixed with a magnetic stirrer for 2 h to achieve desirable homogenization. After drying process, the mixture was crushed for 4 h in a mortar and calcined at 800 °C for 120 min with a heating rate of 2 °C/min. The calcined powder was again milled for 6 h. The obtained fine pow-

der was pressed into discs (pellets) of 13 mm diameter and 1 mm thickness under a pressure of 14000 kg/cm² using a hydraulic press. The pellets were sintered in air at 850, 950, 1050, 1150 and 1180 °C for 2 h in the presence of PbZrO_3 powder, to prevent PbO loss during the high temperature sintering. The sintered pellets were electroded by high-purity silver particle paste, and fired at 750 °C, before any electrical measurements.

X-ray diffraction (XRD, Siemens D500, $\lambda_{\text{CuK}\alpha} = 1.5406 \text{ \AA}$) was used to determine the crystalline phases present in the PZT-PMS ceramics. The compositions of the PZT phases were identified by the analysis of the characteristic XRD peaks of tetragonal (T) and rhombohedral (R) phases, i.e. (002)T, (200)R and (200)T, in the 2θ range 43–46°. Microstructural features such as a grain size and pores were characterized by the scanning electron microscope (SEM) using a FE-SEM Quanta 200 FEG instrument.

Dielectric properties were measured at 1 kHz using an LCR meter (800 GWI, LTD) in the temperature range from 25 to 450 °C with a heating rate of 1 °C/min. The samples used for measurement of piezoelectric properties were poled in a silicone oil bath at 120 °C by applying 30–40 kV/cm for 45 min and then cooled under the same electric field. The piezoelectric properties: piezoelectric constant (d_{31}), electromechanical planar coupling factor (k_p), g_{31} and mechanical quality factor (Q_m) were determined by the resonance and antiresonance technique 24 h after poling, using an impedance analyser (SI1260 Impedance/Gain-Phase Analyzer, Solartron, UK).

III. Results and discussion

3.1. Structure

It has been reported in the literature [20,21] that the dielectric and piezoelectric properties are highly dependent on the density of the ceramics. The density and porosity of the $\text{Pb}[(\text{Zr}_{0.45}, \text{Ti}_{0.5})(\text{Mn}_{0.5}, \text{Sb}_{0.5})_{0.05}]\text{O}_3$ ceramics sintered at various temperatures are presented in Fig. 1. When the sintering temperature was increased from 850 to 1180 °C, the density of the specimens significantly increased and achieved a maximum value at 1180 °C of 97.5% of theoretical value (theoretical density was assumed to be 8.24 g/cm³). The optimal sintering temperature was affected by the addition of impurities and other processing parameters, such as the rate of heating, time of thermal treatment and protecting atmosphere. The optimal sintering temperature was taken as the point when the PbO vapour pressure, evaporation-recondensation equilibrium for the reaction: PbO-PbO (vapour)- Pb (vapour) + $1/2 \text{ O}_2$, was established [22]. It can be noticed that the peak density value corresponds to the lowest value of porosity. Thus, it can be concluded that an optimal sintering temperature of the PZT-PMS specimen is 1180 °C.

Figure 2 shows scanning electron micrographs of the specimens sintered at 1050, 1150 and 1180 °C. From

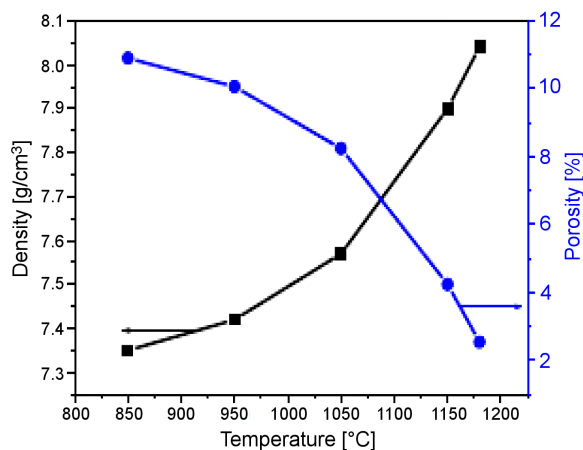


Figure 1. Density and porosity of the PZT-PMS ceramics as a function of sintering temperature

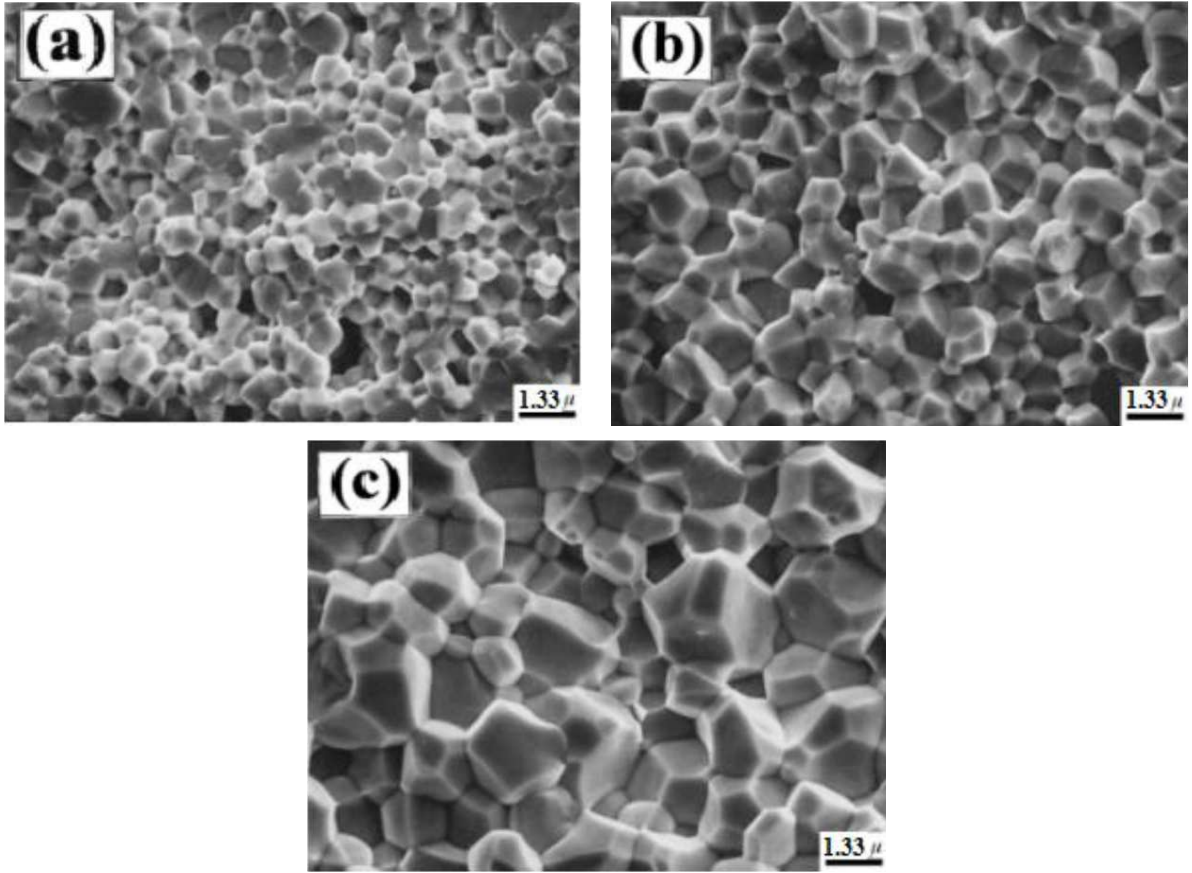


Figure 2. SEM micrographs of PZT-PMS ceramics sintered at: a) 1050 °C, b) 1150 °C and c) 1180 °C

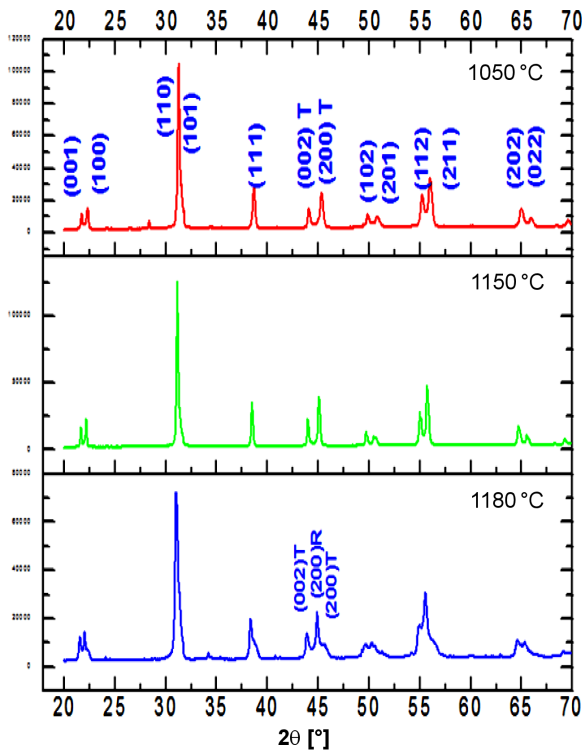


Figure 3. XRD patterns of PZT-PMS ceramics sintered at different temperatures

these images, it can be deduced that there is the decrease of porosity with the increase in sintering temper-

ature, confirmed by obvious decrease in the number and size of pores. Uniform and dense microstructure was obtained at 1180 °C. The average grain size increases with the increase in sintering temperature from 0.75 μm at 1050 °C up to 1.35 μm at 1180 °C. The increase in grain size may have led to the decrease of oxygen vacancies in PZT [23].

To investigate the phase formation and crystal structure, the ceramics was examined by XRD. Figure 3 shows the XRD patterns of the PZT-PMS ceramics sintered at different temperatures from 1050 to 1180 °C. It is observed that the ceramics has perovskite structure without any secondary impurity phases. The samples sintered at 1050 and 1150 °C consist of tetragonal phase, where the {200}-reflections (at 45–46.5°) are associated with tetragonality showing unique splitting [24,25]. The sample sintered at 1180 °C has an extra XRD peak between two tetragonal (200)T and (002)T reflections, indicating the coexistence of tetragonal and rhombohedral phases and formation of MPB after sintering at 1180 °C.

3.2. Dielectric and piezoelectric properties

Figure 4 shows the variation of the dielectric constant as a function of temperature for the PZT-PMS ceramics sintered at 1180 °C measured at the frequency of 1 kHz. The permittivity increases gradually with the increase in temperature and reaches a maximum of 8215 at 345 °C (the Curie temperature). This maximum of dielectric

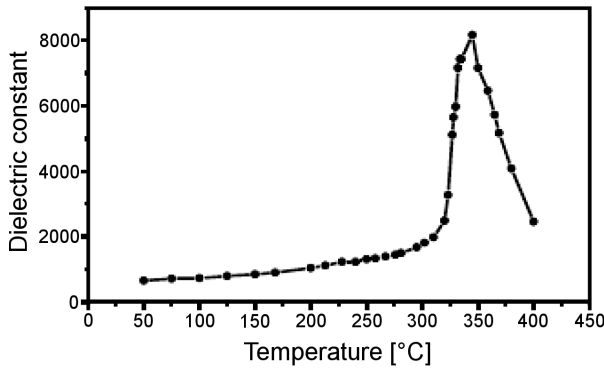


Figure 4. Variation of dielectric constant of PZT-PMS ceramics sintered at 1180 °C as a function of temperature

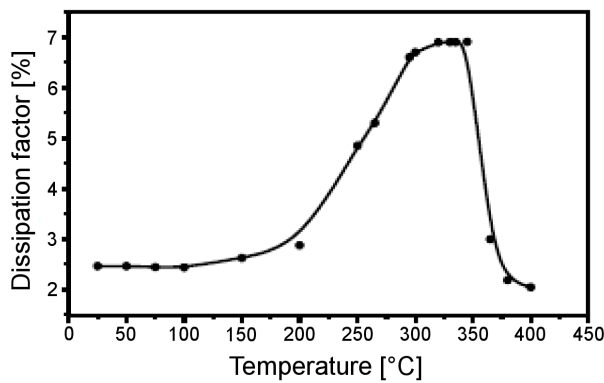


Figure 5. Variation of dissipation factor of PZT-PMS ceramics sintered at 1180 °C as a function of temperature

constant can be explained by the presence of several directions of spontaneous polarization related to the existence of two structures, rhombohedral and tetragonal.

The temperature dependence of loss ($\tan \delta$) for the PZT-PMS ceramics sintered at 1180 °C measured at the frequency of 1 kHz is shown in Fig. 5. The dissipation factor increases with the increase in temperature and then decreases. The maximum of dissipation factor can be explained by the movement of dipole moments. It decreases afterwards with the increase in temperature which causes the deterioration of the material properties.

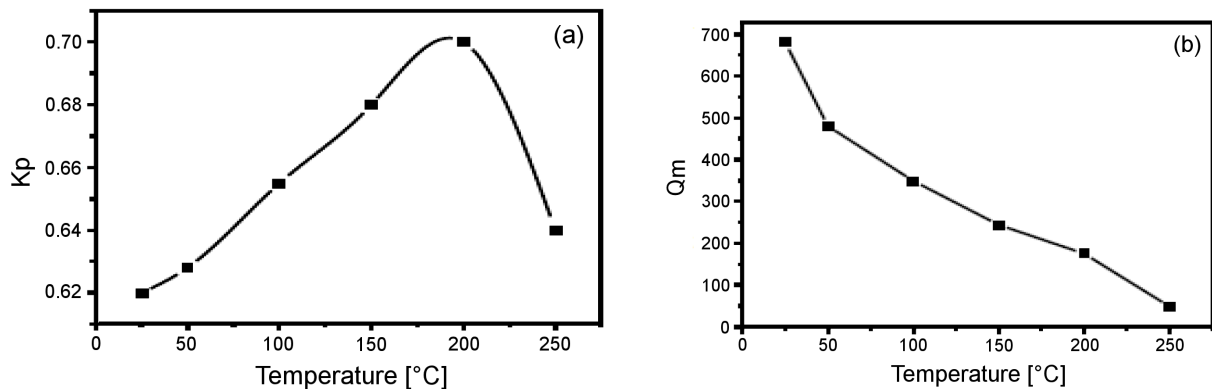


Figure 6. Variations of the planar coupling coefficient k_p (a) and mechanical quality factor (b) of PZT-PMS ceramics sintered at 1180 °C as a function of temperature

The most important property of a piezoelectric material is the electromechanical coupling factor (k_{ij}), which is the figure of merit of the piezoelectric activity. The square of the factor gives the efficiency of the conversion of electrical to mechanical energy [26]. The electromechanical coupling factor has been used as a measure of the piezoelectric response of PZT-type ceramics. It was found that k_{ij} depends on the material parameters such as grain size, porosity and chemical composition [27]. The planar coupling coefficient k_p and mechanical quality factor Q_m were measured for the $\text{Pb}[(\text{Zr}_{0.45}, \text{Ti}_{0.5})(\text{Mn}_{0.5}, \text{Sb}_{0.5})_{0.05}]\text{O}_3$ ceramics sintered at 1180 °C. Variation in the values of the k_p , as a function of temperature is represented in Fig. 6a. The k_p of this system increases as temperature increases and reaches a peak value of 0.70 at 200 °C and then decreases. Usually, the piezoelectric activity increases with the value of the planar coupling coefficient k_p . The variation of the mechanical quality factor along with temperature is shown in Fig. 6b. The Q_m decreases remarkably as temperature increases from 25 to 250 °C. The mechanical quality factor is defined as the reciprocal of the internal friction. Internal friction in the piezoelectric ceramics is due to the movement of domain walls causing the friction between their surfaces. Vacant Pb sites support the movement of domain walls and increase the internal friction within the ceramics, thereby reducing the mechanical quality factor [28].

Variations in the values of the d_{31} , g_{31} and Y as a function of the temperature are represented in Fig. 7. g_{31} increases gradually to its maximum value ($15.9 \cdot 10^{-3} \text{ m}\cdot\text{V}/\text{N}$ at 100 °C) when temperature increases up to a transition temperature (T_{max}) and then decreases. The piezoelectric constant d_{31} increases when the temperature increases, and attains a maximum value of $144.61 \cdot 10^{-12} \text{ C}/\text{N}$ at 250 °C. This maximum of piezoelectric activity can be explained by the presence of several directions of spontaneous polarization related to the existence of the tetragonal and rhombohedral phases. Young's modulus Y decreases continuously when temperature increases from 25 to 250 °C. The decrease of this factor could be explained by the attractive forces that prevent vibration dipoles [29].

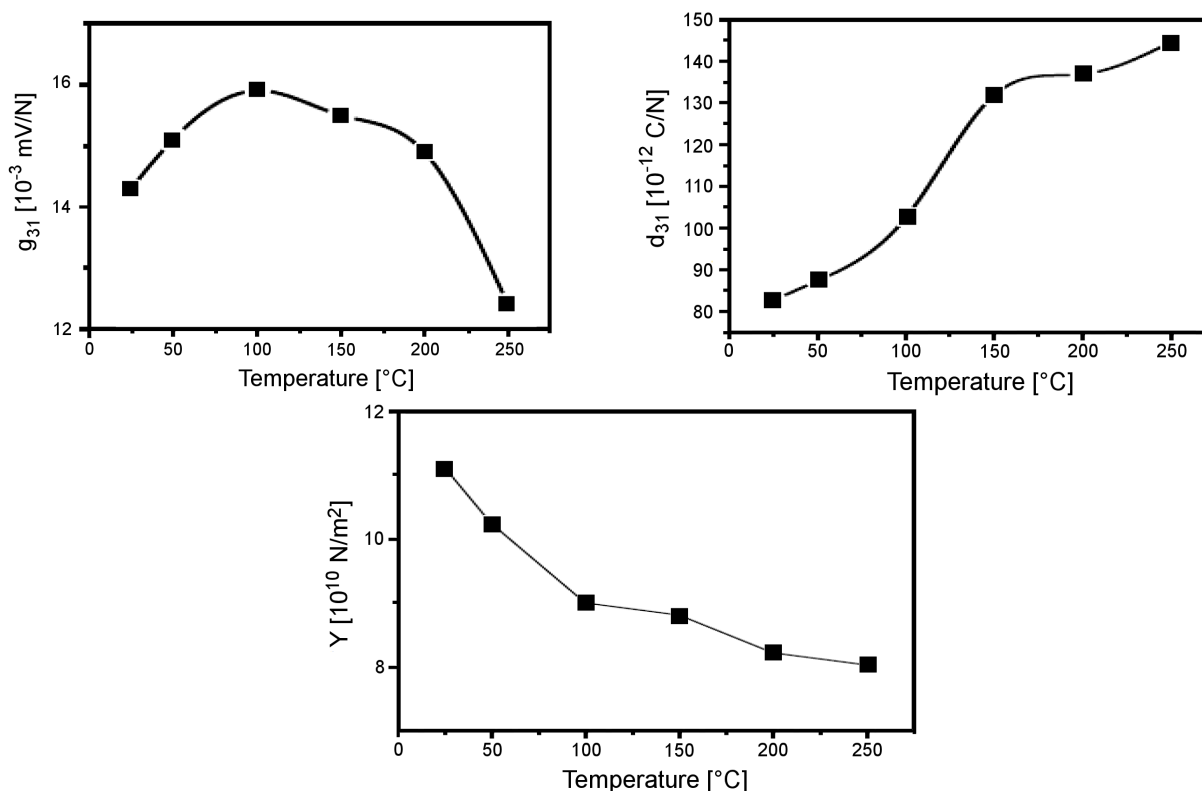


Figure 7. Variations of the piezoelectric constants g_{31} , d_{31} and Young's modulus Y of PZT-PMS ceramics sintered at 1180 °C as a function of temperature

The properties of piezoelectric ceramics can be characterized by three sets of tensor constants: elastic module, piezoelectric constants and dielectric constants. In piezoelectric ceramics, the properties depend on the composition and the crystal structure; the dielectric constant may be increased or decreased through the poling treatment. After poling, the dielectric constant increases for the tetragonal compositions, but decreases for the pseudocubic compositions. The increase of the dielectric constant of the poled tetragonal compositions was previously explained as being due to the elimination of the effect of compression of the 180° domains. In a pseudocubic phase, the dielectric constant decreases after poling, and the net decrease is due to the domain reorientation dominating the effect of the removal of compression [30]. As far as the dielectric constant of polarized ceramics is concerned, its maximum in multi-component systems is displaced into the tetragonal phase, and does not coincide with the maximum of the planar coupling factor. This is, possibly, because of the difference in domain reorientation between these two phases [31].

IV. Conclusions

Sinterability, structure, dielectric and piezoelectric properties of $\text{Pb}[(\text{Zr}_{0.45}, \text{Ti}_{0.5})(\text{Mn}_{0.5}, \text{Sb}_{0.5})_{0.05}]\text{O}_3$ ceramics have been studied. Coexistence of tetragonal and rhombohedral phases was found in the selected composition after sintering at 1180 °C. The region showing the best electrical performance was considered as the core

of MPB. Grain size was in the order of $\sim 1.35 \mu\text{m}$ with the uniform grain size distribution. The PZT-PMS ceramics sintered at 1180 °C has excellent dielectric and piezoelectric properties for wide practical applications. Planar coupling factor of 0.70, poled dielectric constant of 8215, the Curie temperature of 345 °C and a dielectric loss of 6% are attained at 1 kHz and room temperature.

References

1. N. Setter, "Electro-ceramics: Looking ahead", *J. Eur. Ceram. Soc.*, **21** (2001) 1279–1293.
2. R.W. Schwartz, J. Ballato, G.H. Haertling, *Piezoelectric and Electro-optic Ceramics*, pp. 139, Marcel Dekker, New York, 2004.
3. Y. Fang, Y. Xiong, Y.L. Zhou, J.X. Chen, K. Song, Y. Fang, X. Zhen, "Structure and optical properties of cerium(III)-doped PbWO_4 micro-crystals synthesized by a facile wet chemical method", *Solid State Sci.*, **11** (2009) 1131–1136.
4. A. Phuruangrat, T. Thongtem, S. Thongtem, "Synthesis of lead molybdate and lead tungstate via microwave irradiation method", *J. Cryst. Growth*, **311** (2009) 4076–4081.
5. D. Damjanovic, "A morphotropic phase boundary system based on polarization rotation and polarization extension", *Appl. Phys. Lett.*, **97** (2010) 062906.
6. M. Cerqueira, R.S. Nasar, E. Longo, J.A. Varela, A. Beltran, R. Llusar, J. Andres, "Piezoelectric behaviour of PZT doped with calcium: A combined experimental and theoretical study", *J. Mater. Sci.*, **32** (1997) 2381–2386.
7. G. Xu, W. Jiang, M. Qian, X.X. Chen, Z.B. Li, G.R. Han, "Hydrothermal synthesis of lead zirconate titanate nearly free-standing nanoparticles in the size regime of about 4 nm", *Crystal Growth Design*, **9** (2009) 13–16.

8. M. Klee, R. Eusemann, R. Waser, W. Brand, H. Vanhal, "Processing and electrical-properties of $\text{Pb}(\text{Zr}_x\text{Ti}_{1-x})\text{O}_3$ ($x = 0.2-0.75$) films-comparison of metalloorganic decomposition and sol-gel processes", *J. Appl. Phys.*, **72** (1992) 1566–1576.
9. B. Guiffard, E. Boucher, L. Lebrun, D. Guyomar, "Characteristics of F doped PZT ceramics using different fluorine sources", *Mater. Sci. Eng. B*, **137** (2007) 272–277.
10. W. Qiu, H. Hoon Hng, "Effects of dopants on the microstructure and properties of PZT ceramics", *Mater. Chem. Phys.*, **75** (2002) 151–156.
11. Q. Tan, Z. Xu, J.-F. Li, D. Viehland, "Influence of lower-valent A-site modifications on the structure-property relations of lead zirconate titanate", *J. Appl. Phys.*, **80** [10] (1996) 5866–5874.
12. B.W. Lee, E.J. Lee, "Effects of complex doping on microstructural and electrical properties of PZT ceramics", *J. Electroceram.*, **17** (2006) 597–602.
13. A. Garg, D.C. Agrawal, "Effect of rare earth (Er, Gd, Eu, Nd, and La) and bismuth additives on the mechanical and piezoelectric properties of lead zirconate titanate ceramics", *Mater. Sci. Eng. B*, **86** (2001) 134–143.
14. S. Zahi, R. Bouaziz, N. Abdessalem, A. Boutarfaia, "Dielectric and piezoelectric properties of PbZrO_3 - PbTiO_3 - $\text{Pb}(\text{Ni}_{1/3}\text{Sb}_{2/3})\text{O}_3$ ferroelectric ceramics system", *Ceram. Int.*, **29** (2003) 35–39.
15. Y. Jeong, J. Yoo, S. Lee, J. Hong, "Piezoelectric characteristics of low temperature sintering $\text{Pb}(\text{Mn}_{1/3}\text{Nb}_{2/3})\text{O}_3 - \text{Pb}(\text{Ni}_{1/3}\text{Nb}_{2/3})\text{O}_3 - \text{Pb}(\text{Zr}_{0.50}\text{Ti}_{0.50})\text{O}_3$ according to the addition of CuO and Fe_2O_3 ", *Sensors Actuat. A Phys.*, **135** (2007) 215–219.
16. P. Jaita, A. Watcharapasorn, S. Jiansirisomboon, "Effect of BNT addition on microstructure and mechanical properties of PZT ceramics", *J. Microsc. Soc. Thailand*, **24** [1] (2010) 21–24.
17. Y. Yan, K.H. Cho, S. Priya, "Role of secondary phase in high power piezoelectric PMN-PZT ceramics", *J. Am. Ceram. Soc.*, **94** (2011) 4138–4141.
18. Y. Hou, M. Zhu, F. Gao, H. Wang, B. Wang, H. Yan, C. Tian, "Effect of MnO_2 addition on the structure and electrical properties of $\text{Pb}(\text{Zn}_{1/3}\text{Nb}_{2/3})_{0.20}(\text{Zr}_{0.50}\text{Ti}_{0.50})_{0.80}\text{O}_3$ ceramics", *J. Am. Ceram. Soc.*, **87** (2004) 847–850.
19. L.X. He, C.E. Li, "Effects of addition of MnO on piezoelectric properties of lead zirconate titanate", *J. Mater. Sci.*, **35** (2000) 2477–2480.
20. S.Y. Chu, T.Y. Chen, I.T. Tsai, W. Water, "Doping effects of Nb additives on the piezoelectric and dielectric properties of PZT ceramics and its application on SAW device", *Sensors Actuat. A Phys.*, **113** (2004) 198–203.
21. P. Wang, Y. Li, Y. Lu, "Enhanced piezoelectric properties of $(\text{Ba}_{0.85}\text{Ca}_{0.15})(\text{Ti}_{0.9}\text{Zr}_{0.1})\text{O}_3$ lead-free ceramics by optimizing calcination and sintering temperature", *J. Eur. Ceram. Soc.*, **31** [11] (2011) 2005–2012.
22. I. Angus, J. Kingon, C. Brian, "Sintering of PZT ceramics: II, Effect of PbO content on densification kinetics", *J. Am. Ceram. Soc.*, **66** [4] (1983) 256–260.
23. O. Ohtaka, R. Von Der Mühlh, J. Ravez, "Low-temperature sintering of $\text{Pb}(\text{Zr},\text{Ti})\text{O}_3$ ceramics with the aid of oxyfluoride additive: X-ray diffraction and dielectric studies", *J. Am. Ceram. Soc.*, **78** [3] (1995) 805–808.
24. J. Wu, D. Xiao, W. Wu, Q. Chen, J. Zhu, Z. Yang, J. Wang, "Composition and poling condition-induced electrical behavior of $(\text{Ba}_{0.85}\text{Ca}_{0.15})(\text{Ti}_{1-x}\text{Zr}_x)\text{O}_3$ lead-free piezoelectric ceramics", *J. Eur. Ceram. Soc.*, **32** (2012) 891–898.
25. D. Fu, M. Itoh, S. Koshihara, T. Kosugi, S. Tsuneyuki, "Anomalous phase diagram of ferroelectric $(\text{Ba,Ca})\text{TiO}_3$ single crystals with giant electromechanical response", *Phys. Rev. Lett.*, **100** [22] (2008) 227601.
26. K.H. Hartal, "Physics of ferroelectrics ceramics used in electronic devices", *Ferroelectrics*, **12** (1976) 9–19.
27. K. Okazaki, K. Nagata, "Effects of grain size and porosity on electrical and optical properties of PLZT ceramics", *J. Am. Ceram. Soc.*, **56** (1973) 82–86.
28. P. Ari-Gur, L. Benguigui, "X-ray study of the PZT solid solutions near the morphotropic phase transition", *Solid State Commun.*, **15** [6] (1974) 1077–1079.
29. A. Boutarfaia, S.E. Bouaoud, "Tetragonal and rhombohedral phase co-existence in the system: PbZrO_3 - PbTiO_3 - $\text{Pb}(\text{Fe}_{1/5},\text{Ni}_{1/5},\text{Sb}_{3/5})\text{O}_3$ ", *Ceram. Int.*, **22** [4] (1996) 281–286.
30. E.G. Fesenko, A. Ya. Dantsiger, L.A. Resnitohenko, M.F. Kupriyanov, "Composition-structure-properties dependences in solid solutions on the basis of lead-zirconate-titanate and sodium niobate", *Ferroelectrics*, **41** (1982) 137–142.
31. V.A. Isupov, Yu.E. Stolypin, "Coexistence of phases in lead zirconate-titanate solid solutions", *Sov. Phys. Solid State*, **12** (1970) 2067–2071.